Journal of Radiation Research and Applied Sciences 8 (2015) 354–361

HOSTED BY

Available online at www.sciencedirect.com

ScienceDirect

Journal of Radiation Research and Applied Sciences

journal homepage: http://www.elsevier.com/locate/jrras

An estimate of the surface heat fluxes transfer of the Persian Gulf with the overlying atmosphere

A. Rezaei-Latifi [a,*], F. Hosseinibalam [b]

[a] Physics Department, Faculty of Sciences, Hormozgan University, Hormozgan, Bandar Abbas, Iran

[b] Physics Department, Faculty of Sciences, University of Isfahan, Isfahan, Iran

ARTICLE INFO

Article history:
Received 15 November 2014
Received in revised form
23 January 2015
Accepted 5 February 2015
Available online 18 February 2015

Keywords:
Turbulent fluxes
Longwave radiation
Atmosphere
Persian Gulf

ABSTRACT

The ocean heat exchange process is a key mechanism in climate variations over a broad time – scale. In this study, the long–term mean surface heat fluxes over the Persian Gulf have been estimated by the empirical relations using data derived from National Oceanic and Atmospheric Administration (NOAA). The basin-averaged annual mean values of heat transfer due to solar radiation, sensible heat flux, long-wave radiation flux and latent fluxes are about 219,−14, −75 and −136, respectively. Therefore, the long – term annual mean net heat flux is about −6 W m^{-2} (negative sign means upward heat flux) and shows a very good agreement with the direct measured advective value through the Hormuz Strait. The spatial distribution of the surface heat fluxes, which has not been investigated before, show relatively large spatial variation in latent heat flux. The annual mean net heat flux spatial distribution varies from about −30 to 10 W m^{-2}, with greatest heat loss in south-eastern and northwestern regions of the Gulf. In mid – winter (January), the northern region along the Iranian coast loses heat (about 20–80 W m^{-2}) but southern and north-western shallow regions gain heat (about 15 W m^{-2}) from the atmosphere. In mid-summer (July) the spatial variation in net heat flux is weak and is positive at most all over the Gulf.

1. Introduction

The Persian Gulf (Fig. 1) is a shallow, semi-enclosed basin situated in an arid zone with a mean depth of about 36 m where evaporation greatly exceeds precipitation and river runoff. Circulation in the Persian Gulf is dominated by density – driven currents, which are generated and sustained by evaporative losses and radiative heat transfer and slightly by freshwater inflow at the head of the Gulf. These features lead to an inverse estuarine circulation with a fresh surface inflow from Gulf of Oman and a highly saline water leaving the Gulf through the deep part of the Hormuz Strait.

Accurate information of surface heat flux is needed to describe the air – sea interaction. It is indispensable for modeling of the ocean and atmosphere circulation being used as the thermal boundary condition (Hirose & Kim Yoon, 1996). The heat budget for a semi – enclosed sea such as the Persian Gulf, is determined by the net flow of heat entering or leaving the system. The components of the heat budget include terms which define heat conduction through the solid boundaries, heat transfer between the atmosphere and the sea surface,

* Corresponding author.
E-mail address: R_Latifi@hormozgan.ac.ir (A. Rezaei-Latifi).
Peer review under responsibility of The Egyptian Society of Radiation Sciences and Applications.
http://dx.doi.org/10.1016/j.jrras.2015.02.002

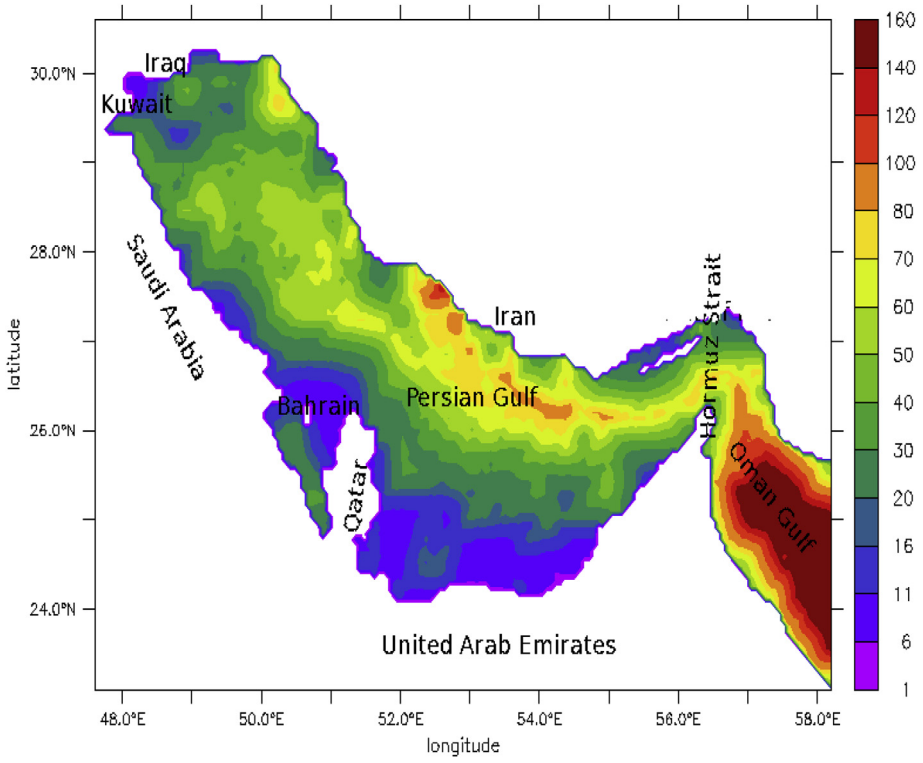

Fig. 1 – Bathymetry (meter) and map of the Persian Gulf.

and advective heat fluxes through the Strait communicating with the exterior. The surface heat fluxes are made up of solar radiation, the loss due to long wave radiation, the loss/gain due to evaporation/condensation and the loss/gain due to conduction.

Based on long – term moored time series observations at the strait of Hormuz, Johns et al. (2003) investigated the water exchange between the Persian Gulf and Indian Ocean. Their calculations of the advective heat and freshwater flux through the Strait led to estimates of 1.68 ± 0.39 m/yr for the net evaporation over the Gulf and a net annual heat loss over the Gulf of -7 ± 4 W m^{-2}. Basin-averaged annual mean heat flux derived from the SOC (Southampton Oceanography Centre) field gave an ocean gain of $+53$ W m^{-2}. Since there was a significant discrepancy between this result and the basin-averaged loss of -7 ± 4 W m^{-2} derived from estimate of advective fluxes through the Hormuz Strait, Johns et al. (2003) corrected the SOL flux estimate and obtained a revised value of the climatological basin mean net heat flux of 4 W m^{-2}. The positive value means that the Persian Gulf gains the heat at the air – sea surface and then out through the Strait Hormuz.

In this work, the heat flux components are evaluated by using empirical relations described in Section 2 and then seasonal and spatial variability of net surface heat flux over the Persian Gulf is investigated. The results of the net heat flux are used to estimate the net heat transport through the Strait of Hormuz.

The rest of this paper is organized as follows. In the next section, the basic formulate for the heat budget and data source are explained. The result of calculations of the surface heat fluxes over the Persian Gulf are described in Section 3. The last section gives the summary and discussion for this paper.

2. Materials and methods

2.1. *Basic formulate*

The different components of the heat flux at the sea surface are:

1. Insolation Q_s, the flux of solar energy into the sea.
2. Net Infrared Radiation Q_b, net flux of long – wave radiation from the sea surface.
3. Sensible Heat Flux Q_h, the turbulent transport of temperature across the air/sea interface.
4. Latent Heat Flux Q_e, the flux of energy carried by evaporated water.

In this paper the sign convention for heat flux components is that upward heat flow from the sea to the atmosphere is negative, while the downward heat flux from atmosphere to sea is positive. Then, the net heat flux through the sea surface Q_{net} is expressed as,

$$Q_{net} = Q_s + (Q_b + Q_h + Q_e) \quad (1)$$

The turbulent heat flux (Q_e, Q_h) is calculated by the bulk formulas:

$$Q_e = -\rho_a L_v C_E W (q_s - q_a) \quad (2)$$

$$Q_h = -\rho_a c_p C_H W(T_s - T_a) \quad (3)$$

where T_s and T_a are the sea surface and air temperature, W is the wind speed at the reference height of 10 m, ρ_a is the density of air, L_v is the latent heat of evaporization, C_E and C_H are latent and sensible transfer coefficients, q_s and q_a are the sea surface and air humidities andc_p is the specific heat of air at constant pressure.

The coefficients of exchange C_H and C_E play an important role in the calculation of the evaporative and sensible heat fluxes. These coefficients depend on wind speed and thermal stratification. Based on Monin – Obukhov similarity theory as described in Geernaert (1990) and Luyten and Mulder (1992) and using monthly averages of air – sea temperature difference and wind speed in the Persian Gulf, the Coefficients are selected as below

$$C_E = C_H = 1.2 \times 10^{-3}$$

The specific heat of air at constant pressure is calculated by using

$$c_p = 100406\ (1 + 0.8375 q_a) \quad (4)$$

The latent heat of evaporization is given as a function of sea surface temperature by the following formula:

$$L_v = 2.5008 \times 10^6 - 2300 T_s \quad (5)$$

The sea surface and air humidities q_s and q_a can be found by using

$$q = \frac{0.62e}{P_{a0} - 0.38e} \quad (6)$$

where $P_{a0} = 1013.25$ mb is reference atmospheric pressure.

The vapor pressure e is obtained in mb from the empirical relation of Gill (1982):

$$\log_{10} e = \log_{10} RH + \frac{0.7859 + 0.03477T}{1 + 0.00412T} \quad (7)$$

where RH is the relative humidity (between 0 and 1). In Equations (6) and (7) the humidity q, vapor pressure e and the temperature T either represent sea surface or atmospheric values at the reference height.

The formula given by Gill (1982) is used to estimate the upward long – wave radiation flux:

$$Q_l = -\varepsilon_s \sigma_{rad} (T_s + 273.15)^4 \left(0.39 - 0.05 e_a^{\frac{1}{2}}\right)\left(1 - 0.6 f_c^2\right) \quad (8)$$

where $\varepsilon_s = 0.985$ is the emissivity at the sea surface, $\sigma_{rad} = 5.67 \times 10^{-8}\ \mathrm{Wm^{-2}k^{-2}}$ Stefan's constant, f_c the fractional cloud cover (between 0 and 1) and e_a the vapor pressure evaluated by using Equation (7).

Taking into account of the effect absorption by the atmosphere, the direct solar radiation incident on the ocean surface, is given by

$$Q_{dir} = Q_t e^{-\tau} \quad (9)$$

where Q_t and τ are the radiation entering at the top of the atmosphere and the extinction factor, respectively. The following form, proposed by Dogniaux (1984 and 1985), is considered for the extinction factor

$$\tau = m_0 \delta_R t_L \quad (10)$$

The optical air mass m_0, Rayleigh's optical thickness δ_R and Linke's factor t_L are expressed as function of the solar altitude γ in degrees, according to

$$\delta_R = (0.9 m_0 + 9.4)^{-1} \quad (11)$$

$$t_L = 0.021\ \gamma + 3.55 \quad (12)$$

$$m_0 = \left[\sin\gamma + 0.15\ (\gamma + 3.885)^{-1.256}\right]^{-1} \quad (13)$$

The formulation, given by Equations (11)–(13), has the advantage that it does not diverge at low solar altitudes.

The direct component of solar radiation must be supplemented by the diffuse sky radiation Q_{dif}. Following Rosati and Miyakoda (1998) it is assumed that one half of the scattered radiation reaches the ocean surface so that

$$Q_{dif} = \frac{1}{2}((1 - A_\alpha) Q_t - Q_{dir}) \quad (14)$$

They considered the value of 0.09 for the water vapor and ozone absorption coefficient A_α. The total radiation flux at the ocean surface under clear sky conditions is then given by

$$Q_{cs} = Q_{dir} + Q_{dif} = \frac{1}{2} Q_t \left(e^{-\tau} + 1 - A_\alpha\right) \quad (15)$$

The clear sky value Equation (15) must be corrected for cloud coverage and for the reflection by the ocean surface. Here, the empirical formula, derived by Reed (1977), is used to correct the clear sky value.

$$Q_s = Q_{cs}(1 - 0.62 f_c + 0.0019 \gamma_{\max})(1 - A_s) \quad (16)$$

where $\gamma_{\max}$ is the solar altitude at noon. A constant value of 0.06 is assumed for the sea surface albedo A_s. It should be noted that we considered integrated the light hours to calculate the solar radiation.

2.2. Data sources

According to the formulae given in Equations (2)–(9), meteorological data, i.e, wind speed, air temperature, relative humidity and cloudiness together with sea surface temperature are required to calculate surface heat fluxes. Monthly mean average Data of 61 years period from 1948 to 2009 were derived from NOAA (National Oceanic and Atmospheric Administration) data. Bathymetry and coastline locations are based on ETOPO-2 data that has been interpolated and slightly smoothed onto a 4-min grid.

The calculations were done using subroutines SURFLX and SOLRAD of physical part COHERENS (Coupled Hydrodynamic Ecological model for Regional Shelf) model (Luyten et. al 1999).

3. Results

3.1. Comparison with SOC air-sea flux climatology

In this section our estimates for basin-averaged annual mean heat flux components are compared against the its evaluated counterpart of the SOC (Southampton Oceanography Centre) fields. The SOC Climatology was developed using various bulk

formulae to estimate the different components of the heat and freshwater exchange from voluntary observing ship meteorological reports in the COADS (Comprehensive Ocean-Atmosphere Data Set) release 1a (Woodruff, Lubker, Wolter, Worley, & Elms, 1993).

Basin-averaged values of the SOC annual mean heat fluxes for the period 1980–1997 with long-wave flux obtained using formula of Clark, Eber, Laurs, Renner, and Saur (1974) are listed in Table 1. Weller, Baumgartner, Josey, Fischer, and Kindle (1998) have suggested that, the evaluations of the SOC fields using data from the meteorological mooring in a neighboring stations of the Arabian Sea are significantly biased by up to 20 W m^{-2} in this region from the Clark et al. (1974) long-wave estimates. Further analysis revealed that long-wave parameterization developed by Bignami, Marullo, Santoleri, and Schiano (1995) using Mediterranean Sea data provides more reliable estimates of the long-wave flux under the conditions of low cloud cover the characteristic of Arabian Sea. Similar accuracy is expected for the Persian Gulf as they are close in nature to the Arabian Sea and the latter formulation is appropriate for estimating climatological net heat fluxes. In addition to the long-wave, the SOC short-wave flux was obtained with Reed (1977) formula, which does not allow for the screening effect of aerosols and thus since the Persian Gulf is a region of strong aerosol loading (Husar, Prospero, & Stowe, 1997) the SOC short-wave estimate may also be biased high. In order to estimate the magnitude of this bias Johns et al. (2003) applied the Tragou, Garrett, and Outerbridge (1999) correction to the original SOC short-wave estimates using AVHRR estimates o the aerosol optical depth. They found a significant adjustment, 37 W/m^2, to the short-wave flux over the gulf, which led to a reduction in the basin-averaged short-wave flux from 248 W m^{-2} to 211 W m^{-2}. Table 2 shows the SOC mean heat fluxes with long-wave flux obtained using the formula of Bignami et al. (1995) and short-wave flux corrected by the Johns et al. (2003). The Basin –averaged annual mean heat flux components computed in this paper, are listed in Table 3. Comparison between Table 2 and Table 3 show that our estimate is relatively close to revised SOC heat flux components. However, there is a discrepancy between SOC heat flux and estimated in this study. While in a good agreement with the advective estimate (Johns et al. 2003) we obtained a negative value of −6 W m^{-2} for net heat flux, the revised SOC net heat flux is a positive value of 4. It appears that this difference is mostly due to bias in the latent heat flux. The SOC heat latent flux is significantly smaller in magnitude than our result and previous regional studies. The lower value of the net evaporation from the SOC climatology could be largely attributed to under sampling in coastal regions of the Gulf, since the marine weather observation upon which these estimate are based are confined mostly to the marine shipping areas in deep water (Johns et al. 2003).

Table 1 – Components of the SOC basin-averaged annual mean heat fluxes with long-wave flux obtained using the formula Clark et al. (1974) for the Gulf, 1980-1997.

Component	value (Wm^{-2})
Latent	−122
Sensible	−7
Longwave: Clark	−59
Shortwave	241
Net heat flux	53

Table 2 – Components of the SOC basin-averaged annual mean heat fluxes with long-wave flux obtained using the formula Bignami et al. (1995) *and* short-wave flux corrected by Johns et al. (2003).

Component	value (Wm^{-2})
Latent	−122
Sensible	−7
Longwave: Bignami	−78
Shortwave: Carected	211
Net heat flux	4

3.2. *Surface heat fluxes*

The result of calculations of basin – averaged heat fluxes at the air – sea interface are given in Fig. 2 and Table 4. The positive values of the sensible heat flux Q_h, occur from April through June as a result of positive difference of the sea-air temperature (air warmer than the water). For the other months of the year the air is colder than sea surface water and,hence, the sensible heat flux is negative (b in Fig. 2 and Table 4). The latent heat flux Q_e varies considerably during the year, being more negative in summer and less negative lower in winter (d in Fig. 2 and Table 4). This is not in agreement with Privett (1959) results where evaporation is higher in winter. The examination of NOAA data shows that the monthly mean wind speed is stronger in summer months than any other time. Besides, the air humidity decreases significantly in summer. Thus, these seemed to cause greater evaporation in summer. Negative values of Q_e occur in all months, reflecting the fact that on the average sea – air vapor pressure differences are positive throughout the year. The upward long – wave radiation flux Q_b varies from −70 to −82 W/m^2 and its magnitude is larger than Q_h but smaller than Q_e during the year. It takes a maximum value in May and June due to the relatively low values of cloud cover and large values of sea surface temperature (SST) during these months, while minimum values occur in August and September (c in Fig. 2 and Table 4). The short – wave radiation flux Q_s changes from 110 W m^{-2} to 325 W m^{-2} with its highest value occurs in June (a in Fig. 2). The basin-averaged annual mean values of heat transfer due to radiation, sensible heat, infrared radiation and latent fluxes are about 219,−14, −75 and −136, respectively.

Fig. 3 shows time series of basin – averaged net heat flux. The Q_{net} is positive between February and August and negative

Table 3 – Components of the basin-averaged annual mean heat fluxes estimated in this study.

Component	value (Wm^{-2})
Latent	−136
Sensible	−14
Longwave	−75
Shortwave	219
Net heat flux	−6

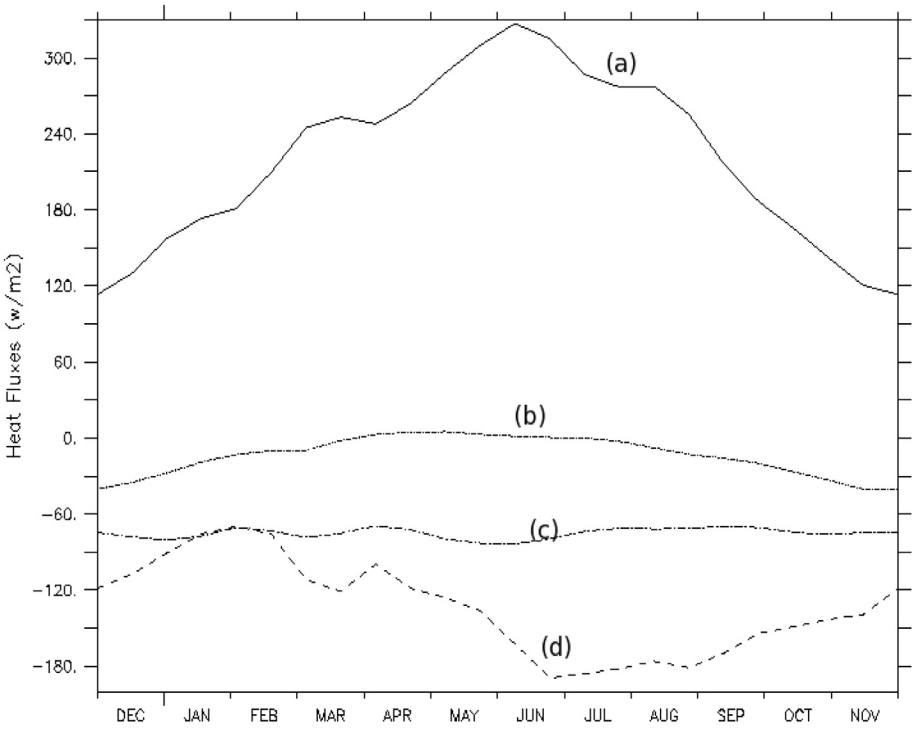

Fig. 2 – Time series of the basin – averaged heat fluxes for a) short - wave radiation b) sensible c) long - wave radiation and d) latent. negative value indicates that sea loses heat to air. The calculations were initialized in early winter (December).

in the other months of the year. Thus, the Persian Gulf gains heat in February–August and loses in other months at the air – sea interface. The annual net heat flux varies from −91 W m^{-2} in May to −127 W m^{-2} in November. The annual mean value of Q_{net} over the Persian Gulf is about −6 W m^{-2}, which indicates a net heat loss from the sea to the atmosphere. This is in good agreement with the value estimated by Johns et al. (2003). Since the magnitude of heat transport from rivers to the Gulf seems to be negligible, the net heat loss at the air – sea interface must be compensated by the net flow of heat entering the Gulf through Hormuz Strait.

Fig. 4 shows long – term annual mean distribution of latent heat flux Q_e, sensible heat flux Q_h, long – wave radiation flux Q_b and net heat flux Q_{net}. There is relatively large spatial variability in Q_e(a in Fig. 4) compared to Q_h (b in Fig. 4) and Q_b (c in Fig. 4). This is mostly due to considerable spatial variability of sea surface vapor pressure, especially in winter and autumn. The magnitude of Q_e in southern shallow regions, contrary to Q_h, is larger than northern deep regions along the Iranian coast. The annual mean sensible heat flux varies from about −10 W m^{-2} in south to −18 W m^{-2} in small portion along the Iranian coast, but at most parts of the Gulf is about – 15 W/m^2. The magnitude of Q_b is about 75 W m^{-2} and is almost uniform all over parts of the Gulf. The annual mean of the net heat flux varies from −30 W m^{-2} to 10 W m^{-2}at most parts of the Gulf and the maximum heat loss occurs mostly in the southern and west part.

Table 4 – Monthly averages of short wave radiation Q_s, long wave radiation Q_b, sensible heat flux Q_h, latent heat flux Q_e, and net heat flux Q_{net}. (Unit is Wm^{-2}).

Month	Q_s	Q_b	Q_h	Q_e	Q_{net}
D	122	−76	−37	−115	−106
J	166	−79	−23	−85	−21
F	196	−72	−11	−75	38
M	249	−77	−6	−118	48
A	256	−71	4	−111	78
M	299	−81	4	−133	89
J	321	−82	1	−179	61
J	281	−72	−1	−186	22
A	266	−71	−10	−181	4
S	202	−70	−18	−163	−50
O	154	−75	−30	−149	−99
N	118	−74	−41	−136	−133

Fig. 5 indicates spatial distribution of the long – term monthly mean net heat flux. In January (a in Fig. 5), Q_{net} is negative for most parts of the Gulf. The northern deep region of the Gulf shows a maximum heat loss and it reaches about 60 W m^{-2}. The southern and northwestern shallow regions along the United Arab Emirates (UAE), Bahrain and Kuwait coasts gain heat about 20 W m^{-2}. This variability of the net heat flux is associated with relatively large spatial change of SST in winter. The data analysis indicates that sea surface temperature over the southern shallow reigns is about 5 °C lower than northern deep parts in January. The In April (b in Fig. 5), the overall regions of the Gulf gain heat from the atmosphere. The net heat gain is from about 20 to 40 W m^{-2}. Its maximum occurs in the deep region along the Iranian coast and it is a minimum value over the southern region along the UAE and Bahrain coasts. In July (c in Fig. 5), there is little

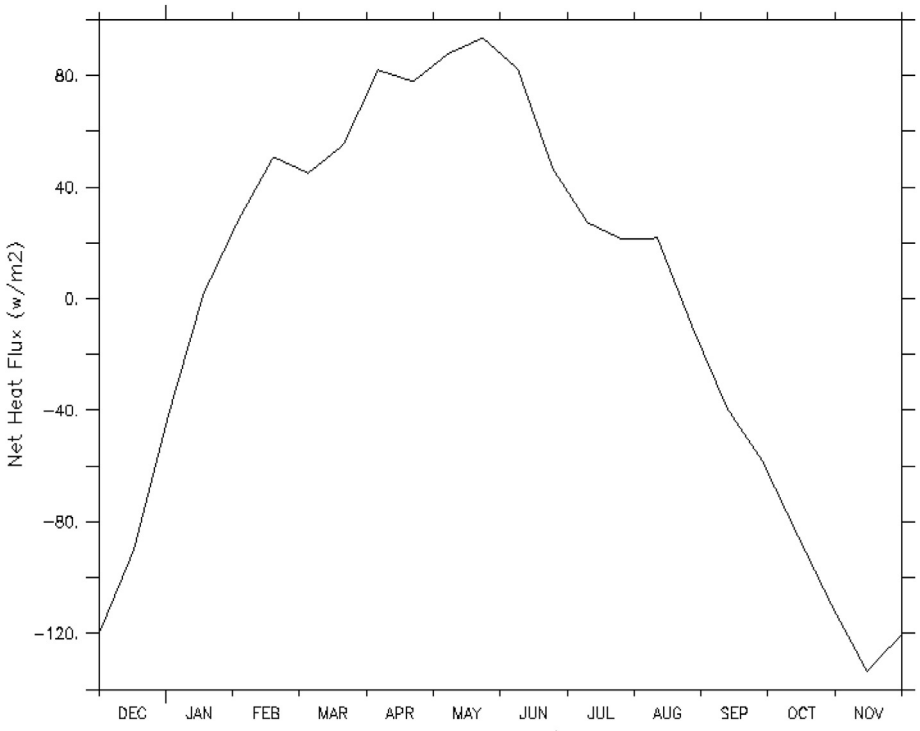

Fig. 3 – Time series of the basin – averaged net heat flux. negative value indicates that sea loses heat to air. (Unit is Wm^{-2}).

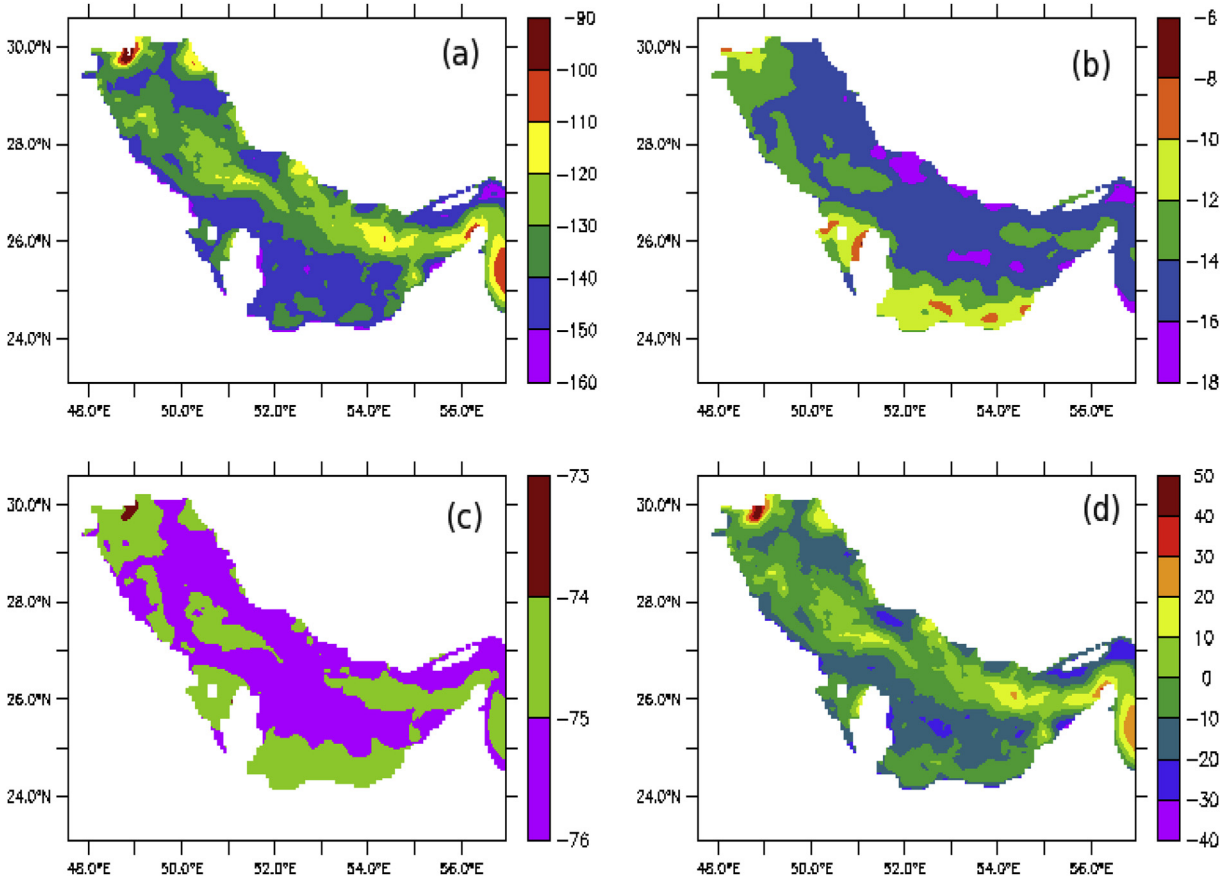

Fig. 4 – Annual mean distributions of a) latent heat flux Q_e b) sensible heat flux Q_h c) long – wave radiation flux Q_b and d) net heat flux. Negative value indicates that the sea loses heat to air. (Unit is Wm^{-2}).

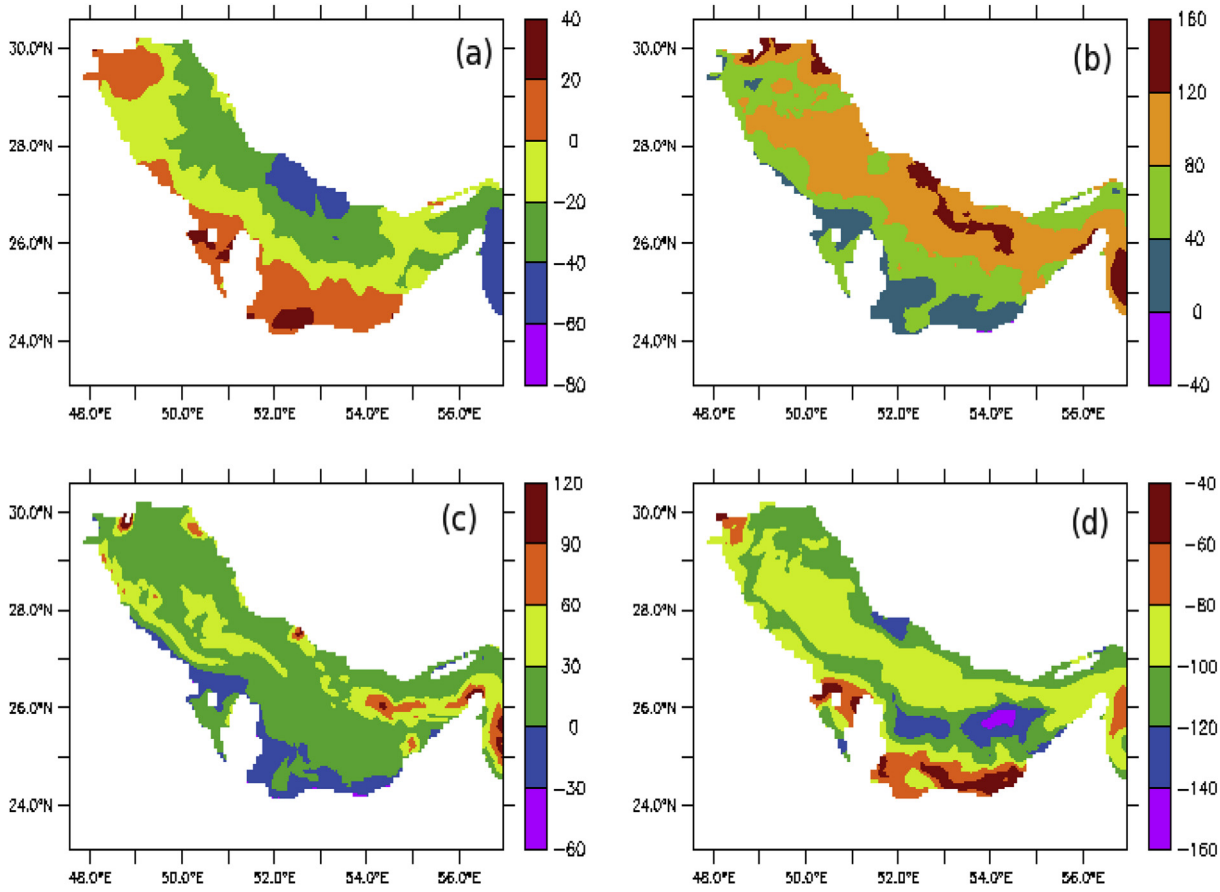

Fig. 5 – Spatial distribution of the long – term monthly mean net heat flux in a) January b) April c) July and d) October (Unit is Wm^{-2}). Negative value indicates that the sea loses heat to air.

spatial variation in Q_{net} and the Persian Gulf gains heat from the atmosphere except for small areas at the southern and west part. During these months, the heat gain is relatively small (about 20 W m^{-2}) compared to April. In October (d in Fig. 5), Q_{net} is negative, namely, the heat loss occurs all over the Persian Gulf. Its magnitude varies from 40 W m^{-2} at southern region along the UAE and Bahrain coasts to 160 W m^{-2} at deepest region in the southern part.

It is interesting to note that although the period of heat gain (seven months) is longer than heat loss (five months), the annual mean net heat flux is negative.

The reason for this is that the basin-averaged net heat flux is more negative in period of heat loss but is less positive during the heat gain. More negative values of Q_{net} is produced by a large decrease in the solar heating and relatively large values Q_e and Q_b in the balance.

4. Conclusion

The assumption that an enclosed sea attains a steady state over long enough periods of time can be used to check the consistency of empirical expressions by comparing the net surface heat transfer to the independently and directly measured advective value. In this work, the Bulk Aerodynamic method and the formula given by Gill (1982) were used to estimate the turbulent fluxes (Q_h and Q_e) and the net backward longwave radiation, respectively. The Rosti and Miyakoda approach was followed to estimate the short-wave radiation at the ocean surface under clear sky condition and then it was corrected for the reflecting by the ocean surface using the empirical formula derived by Reed (1977). By using these empirical relations the values of −14, −136, 219 and −75 W m^{-2} were obtained for basin-averaged annual mean fluxes of the sensible, latent, shortwave and longwave radiation. The net surface heat transport over the Persian Gulf Q_{net} is −6 W $m^{-2}$and the maximum heat loss occurs in November. Since the magnitudes of heat transport from rivers run-off and precipitation to the Persian Gulf are small and negligible, this net heat loss at the air-sea interface must be compensated by the net flow of heat entering the Gulf through Hormuz Strait. This result is in a good agreement with advective budget estimated by Johns et al. (2003). Moreover, it appears that our estimation of Q_{net} is more reasonable than the SOC climatology estimate because the SOC mean net heat flux is positive and this is disagreement with the directly measured advective value and previous regional studies. It should be noted that net heat flux is strongly seasonal and while its annual mean is negative, the time period of heat gain (February–August) is longer than heat loss

(September–January). Seasonal variability in net surface heat flux is largely associated with the insolation Q_s and latent heat loss Q_e . The net heat flux reaches zero value in January and August (Fig. 3) so that these months correspond to the transition periods of the surface heat budget in the Persian Gulf.

In winter, the large spatial variability in SST causes the net heat gain from the southern shallow regions but heat loss over northern deep parts. In spring and summer, due to solar heating almost all over the gulf gains the heat from the atmosphere and maximum net heat gain occurs over the northern deep parts because of lower evaporation in these regions. In autumn all areas of the Persian Gulf lose heat from the sea to the overlying atmosphere because of decrease of solar radiation and relatively large amount of evaporation. The spatial distribution of the annual mean net heat flux indicates that most areas of the Persian Gulf lose heat from the sea to the overlying atmosphere in total. The maximum heat loss occurs in the southern shallow regions close to UAE and around Bahrain together with northwestern part along the Iranian coast.

REFERENCES

Bignami, F., Marullo, S., Santoleri, R., & Schiano, M. E. (1995). Longwave radiation budget in the Mediterranean Sea. *Journal of Geophysical Research, 100*, 2501–2514.

Clark, N. E., Eber, L., Laurs, R. M., Renner, J. A., & Saur, J. F. T. (1974). *Heat exchange between ocean and atmosphere in the eastern North Pacific for 1961-71*. NOAA Tech. Rep. NMFS SSRF-682. 108 pp. Natl. Oceanic and Atmos. Admin., Silver Spring, Md

Dogniaux, R. (1984). Eclairement energetique solaire direct diffuse et global des surfaces orientees et inclinees. Part I: algorithmes et methodologies. *Miscellanea Serie B,* 59, 46 pp.

Dogniaux, R. (1985). Programme general de calcul des eclairements solaires energetiques et lumineux des surface orientees et inclinees. Ceils clairs, couverts et variables. *Miscellanea Serie C, 21*, 37 pp.

Geernaert, G. L. (1990). Bulk parameterizations for the wind stress and heat fluxes. In W.J. Plant (Series Ed.) & G. L. Geernaert (Vol. Ed.), *Current theory: Vol. 1. Surface waves and fluxes*. Kluwer Academ.

Gill, A. E. (1982). Atmosphere-ocean dynamics. In *International geophysics series, 30*Orlando: Academic Press, 662 pp.

Hirose, N. C. H., & Kim Yoon, J. H. (1996). Heat budget in the Japan Sea. *Journal of Oceanography, 52*, 553–574.

Husar, R. B., Prospero, J. M., & Stowe, L. L. (1997). characterization of tropospheric aerosols over the oceans with the NOAA advanced very high resolution radiometer optical thickness operational product. *Journal of Geophysical Research, 102*.

Johns, W. E., Yao, F., Olson, D. B., Josey, S. A., Grist, J. P., & Smeed, D. A. (2003). Observation of seasonal exchange through the straits of Hormuz and the inferred freshwater budgets of the Persian Gulf. *Journal of Geophysical Research, 108*(C12), 3391,. http://dx.doi.org/10.1029/2003JC001881.

Luyten, P. G., Jones, J. E., Proctor, R., Tabor, A., Tett, P., & Wil-Allen, K. (1999). *COHERENS — a coupled hydrodynamical — ecological model for regional and shelf seas: Usr documentation.* MUMM Rep., Management Unit Mathematical Models of the north sea.

Luyten, P. J., & Mulder, T. D. (1992). *A module representing surface fluxes of momentum and heat*. Technical Report No. 9 MAST-0050-C (MUMM), 30 pp.

Privett, D. W. (1959). Monthly charts of evaporation from the N. Indian Ocean (Including the Red Sea and the Persian Gulf. *Quarterly Journal of the Royal Meteorological Society, 8*, 5709–5725.

Reed, R. K. (1977). On estimating insolation over the ocean. *Journal of Physical Oceanography, 7*, 482–485.

Rosati, A., & Miyakoda, K. (1998). A general circulation model for upper ocean simulation. *Journal of Physical Oceanography, 18*, 1601–1626.

Tragou, E., Garrett, C., & Outerbridge, R. (1999). The heat and freshwater budgets of the Red Sea. *Journal of Physical Oceanography, 29*, 2504–2522.

Weller, R. A., Baumgartner, M. F., Josey, S. A., Fischer, A. S., & Kindle, J. (1998). Atmospheric forcing in the Arabian Sea during 1994–1995: observations and comparisons with climatology and models. *Deep-Sea Research Part II, 45*, 1961–1999.

Woodruff, S. D., Lubker, S. J., Wolter, K., Worley, S. J., & Elms, J. D. (1993). Comprehensive ocean- atmosphere data set (COADS) release 1a: 1980–92. *Earth. Monit., 4*, 4–8.